RAFFLES BULLETIN OF ZOOLOGY Supplement No. **36**: 426–434
Date of publication: 6 August 2021
DOI: 10.26107/RBZ-2021-0045
http://zoobank.org/urn:lsid:zoobank.org:pub:04278E32-82EA-4107-B548-084A0484E4A8

Redescription of *Ophiolipus levis* (Echinodermata: Ophiuroidea) collected from deep waters in the Sunda Strait

Masanori **Okanishi**[1*], Takumi **Matsuo**[2,3] & Toshihiko **Fujita**[2,3]

Abstract. *Ophiolipus levis* Koehler, 1904, of the family Ophiosphalmidae is redescribed based on a single specimen from deeper waters in the Sunda Strait, western Indonesia. This is only the second record of the species since its original description. The ossicles under the thick skin were observed for the first time using non-destructive X-ray micro-computed tomography. Detailed observations of external and internal ossicles of this species confirmed its genus and family affiliations.

Key words. brittle star, ossicle morphology, X-ray micro-CT, Indonesia, SJADES

INTRODUCTION

The genus *Ophiolipus* (Ophiuroidea: Euryophiurida: Ophiurida: Ophiosphalmidae) was erected by Lyman, 1878, and currently comprises three species: *Ophiolipus agassizii* Lyman, 1878, *O. granulatus* Koehler, 1897, and *O. levis* Koehler, 1904 (Stöhr et al., 2020). However, these three species have rarely been collected and the detailed morphology of *Ophiolipus* has not been sufficiently investigated. *Ophiolipus levis* Koehler, 1904, is only known from the original description based on two specimens collected from deep waters off eastern Indonesia (Koehler, 1904; see Fig. 1). Although external features with sketches showing diagnostic characters of this species were provided in the original description, no data on ossicle microstructures are available. O'Hara et al. (2018) assigned *Ophiolipus* to the family Ophiosphalmidae together with *Ophiosphalma* H. L. Clark, 1941, and *Ophiomusium* Lyman, 1869, based on phylogenomic and morphological data.

In recent taxonomic descriptions of ophiuroids, it has become standard practice to include details of ossicle microstructure using scanning electron microscopy (SEM), and in some cases also using non-destructive X-ray micro-computed tomography (μCT), which have unlocked characters of critical taxonomic value (e.g., Martynov, 2010; Thuy & Stöhr, 2016; Okanishi et al., 2017; Okanishi & Fujita, 2018).

In this paper, we describe a specimen of *Ophiolipus levis* recently collected by the South Java Deep-Sea (SJADES) Biodiversity Expedition 2018. We seized this opportunity to provide a detailed assessment of the morphology of *O. levis*, including microstructural features of the ossicles using SEM and μCT.

MATERIAL AND METHODS

The specimen was collected during a cruise of RV *Baruna Java VIII* of the Indonesian Institute of Sciences (Lambaga Ilmu Pengetahuan Indonesia, LIPI), as part of the South Java Deep-Sea (SJADES) Biodiversity Expedition 2018. It was fixed in 99% ethanol and deposited in the Museum Zoologi Bogor (MZB), Indonesian Institute of Sciences (LIPI), Cibinong. The voucher number of this specimen is RCO.ECH.3158. An arm of the specimen was dissected to observe its internal ossicles. For observation by scanning electron microscopy (SEM), the ossicles were isolated using domestic bleach (approximately 5% sodium hypochlorite solution), washed in deionised water, dried in air, and mounted on SEM stubs using double-sided conductive tape. The ossicles were examined with a JEOL JSM-5510LV scanning electron microscope.

The entire body of the specimen, immersed in ethanol, was observed by micro-CT, using an inspeXio SMX-225 CT FPD HR (Shimadzu Co. Ltd.), to examine the approximate shapes of a variety of ossicles and their positional arrangements. Scanning parameters were as follows: source voltage: 115kV; source current: 70μA; exposure time for 1 frame: 1 second; total number of views: 1,800; total time for scanning: 30 min; detector size: 1,024 × 1,012 pixel; voxel size: 54 μm. Three-dimensional visualisation was processed with VGSTUDIO MAX3.2 (Volume-Graphs GmbH; https://www.volumegraphics.com/jp/products.html), producing the digital dissection images. The size was measured based on volume

[1]Misaki Marine Biological Station, Graduate School of Science, The University of Tokyo, 1024 Koajiro, Misaki, Miura, Kanagawa, 238-0225, Japan; Email: mokanishi@tezuru-mozuru.com (*corresponding author)

[2]Department of Zoology, National Museum of Nature and Science, 4-1-1 Amakubo, Tsukuba, Ibaraki, 305-0005, Japan

[3]Department of Biological Sciences, Graduate School of Science, The University of Tokyo, 7-3-1 Hongo, Bunkyo, Tokyo, 113-8654, Japan

ISSN 2345-7600 (electronic) | ISSN 0217-2445 (print)

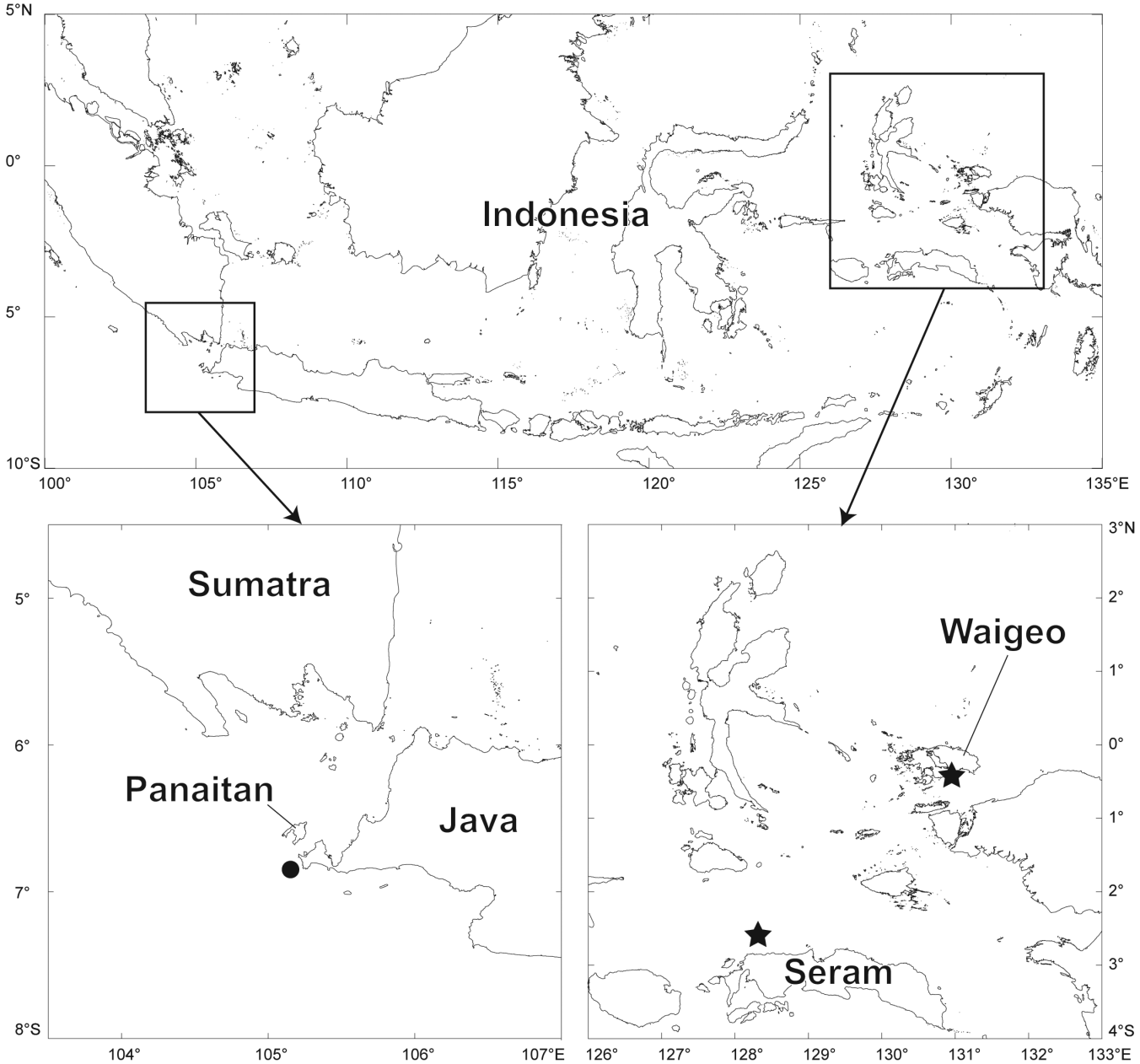

Fig. 1. Distribution of *Ophiolipus levis*. Black circle indicates the collection locality of the specimen examined in this study. Black stars indicate collection localities of two specimens in the original description (Koehler, 1904).

rendering images for the ossicles that could not be measured by external morphological observation due to the covering of thickened skin (e.g., radial shields and other plates on dorsal surface of disc in Fig. 4B). Management and storage of CT data was implemented on figshare (DOI: 10.6084/m9.figshare.14555361).

Morphological terminology used herein follows Stöhr et al. (2012) and Hendler (2018). Hendler (2018) identified oral papillae by numerous terms, based on ontogenetic analyses. In this study, however, we had no data of ontogenetic changes of *Ophiolipus levis*. Thus, we did not distinguish the ossicles on oral plates and adoral shields and used "oral papillae sensu lato" (hereafter "oral papillae s.l.") for the ossicles according to Hendler (2018), and we refer to the ossicles on the dental plate as "teeth". The classification of this species follows O'Hara et al. (2018).

TAXONOMY

Family Ophiosphalmidae O'Hara, Stöhr, Hugall, Thuy & Martynov, 2018

Ophiolipus Lyman, 1878

Ophiolipus levis Koehler, 1904
(Figs. 2–6)

Ophiolypus (sic) *levis* Koehler, 1904: 21, 22, pl. 4 figs. 4–6 (see Remarks).

Material examined. 1 specimen (RCO.ECH.3158), ethanol, collected with a beam trawl, SJADES 2018 st. CP25, south of Panaitan Island, Sunda Strait, Indonesia (6°50.185′S, 105°10.353′E–6°50.923′N, 105°10.776′E), 876–937 m depth, 27 March 2018 (Fig. 1).

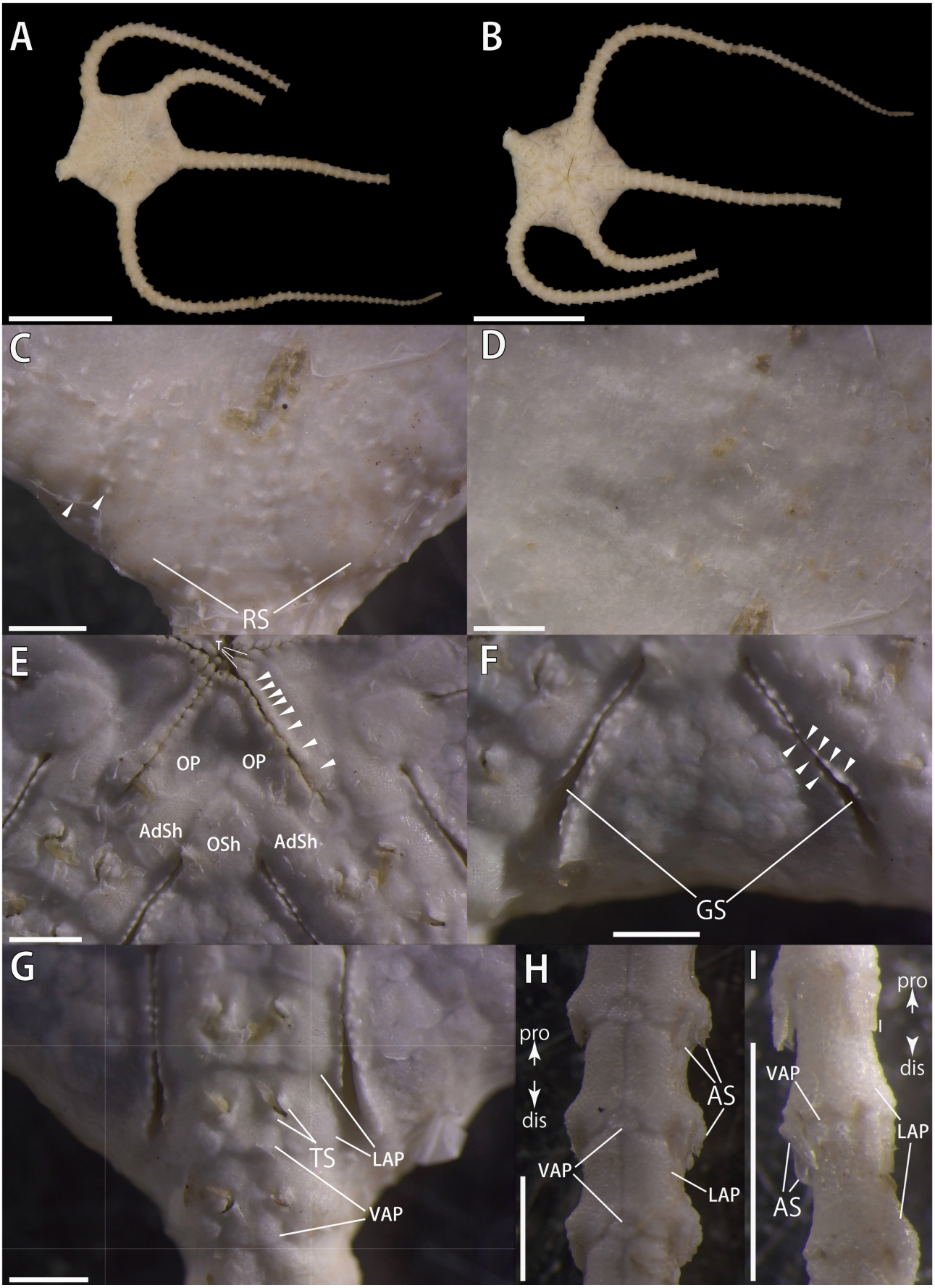

Fig. 2. *Ophiolipus levis*. A, dorsal body; B, ventral body; C, dorsal peripheral disc, arrowheads indicate small granules; D, dorsal central disc; E, ventral disc, arrowheads indicate oral papillae s.l.; F, interradial ventral disc, arrowheads indicate genital papillae; G–I, ventral view of proximal (G), middle (H) and distal (I) portion of arms. Orientations: dis, distal; pro, proximal. Abbreviations: AdSh, adoral shield; AS, arm spine; GS, genital slit; LAP, lateral arm plate; OP, oral plate; OSh, oral shield; RS, radial shield; T, tooth; TS, tentacle scale; VAP, ventral arm plate. Scale bars = 1 cm (A, B); 1 mm (C–I).

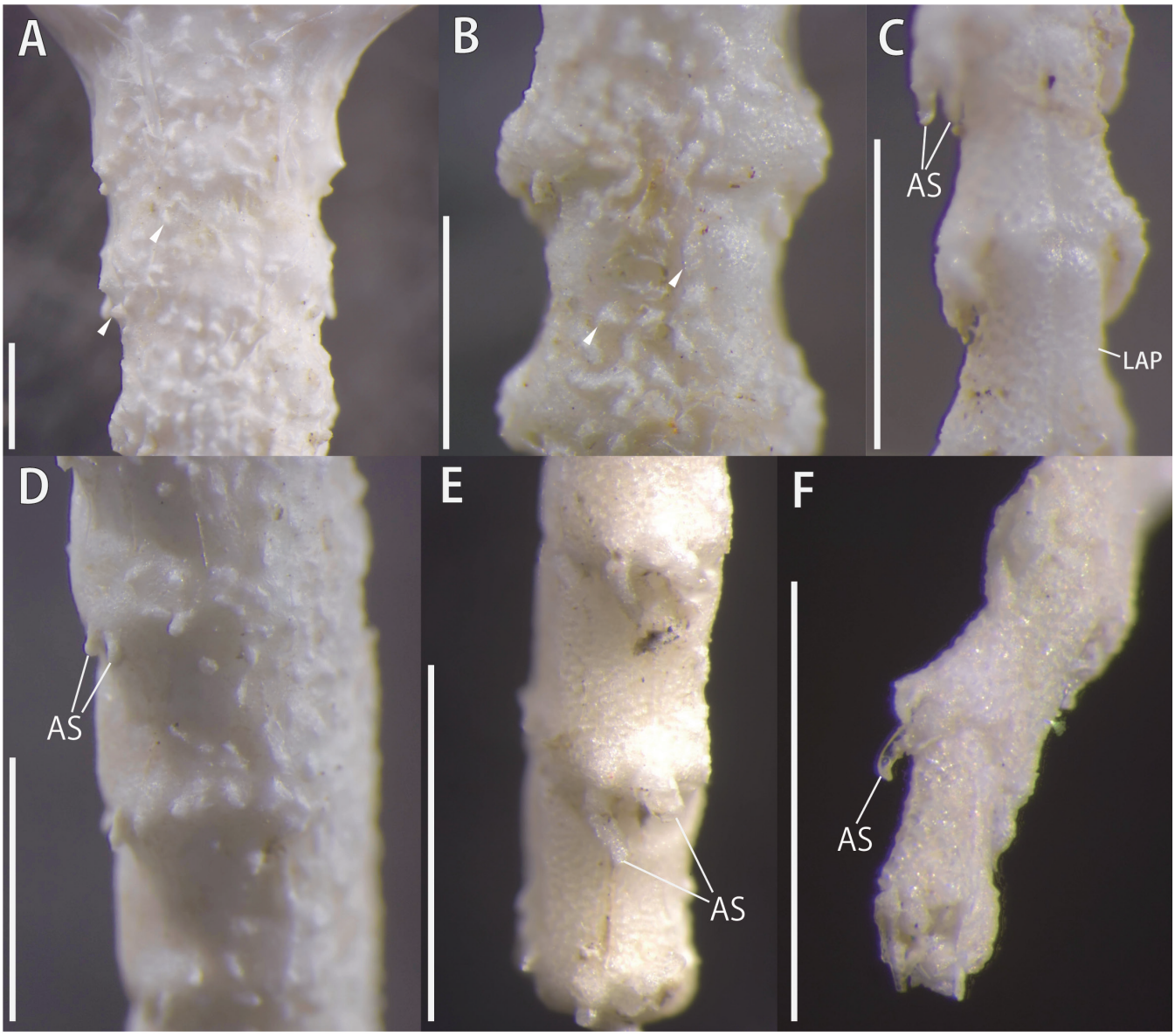

Fig. 3. *Ophiolipus levis*. A–C, dorsal view of proximal (A), middle (B) and distal (C) portion of arms; D–F, lateral view of proximal (D), middle (E) and distal (F) portion of arms. Arrowheads indicate small granules (A, B). Orientation is as follows: upper: proximal; lower: distal side (A–F); left: ventral; right: dorsal (D–F). Abbreviations: AS, arm spine; LAP, lateral arm plate. Scale bars = 1 mm.

Distribution. Indonesia: north of Seram Island and south of Waigeo Island, eastern Indonesia (Koehler, 1904); south of Panaitan Island, Sunda Strait, western Indonesia (this study) (Fig. 1). Depth range 469–937 m.

Diagnosis. Dorsal side of disc and arms covered by skin embedded with small granules separated from each other; oral papillae s. l. five to eight in number on each jaw edge; one hook-shaped arm spine at each tentacle pore in distal portion of arm.

Description. *Disc.* Pentagonal, 13.1 mm in diameter (Fig. 2A). Dorsal surface entirely covered by skin concealing disc ossicles. Small granules present between the skin and the disc ossicles at peripheral disc, circular or slightly oblong in shape, approximately 0.1 mm in diameter, separated from each other (Fig. 2C, D). Radial shields completely concealed by skin, slightly tumid and without granules (Fig. 2C), triangular with an acute angle and a wide distal edge, 1.4 mm in width, 2.0 mm in length, accounting for approximately half of the disc radius (Fig. 4A, B). Radial shields articulated with adradial genital plates at their distal edge on the abradial side of the 4th vertebra (Fig. 4C). Adradial genital plates articulated with abradial genital plates at their distal edge (Fig. 4C). One large plate at each interradial disc margin, approximately 1.6 mm in length (Fig. 4A, B). One central and five radial hemispherical primary plates, approximately 0.7 mm in diameter; several glassy and hemispherical scales, approximately 0.3–0.5 mm in diameter, arranged five-radial symmetrically (Fig. 4A, B). Remaining dorsal surface covered by smaller flat scales under the skin.

Ventral surface entirely covered by skin (Fig. 2B). No granules under the skin. Oral shields pentagonal, slightly round, both lateral edges convex, approximately 1.5 times longer than wide (1.0 mm in width, 1.4 mm in length) (Figs. 2E, 4D). Adoral shields triangular, wider than long, approximately three times wider than long (2.0 mm in width,

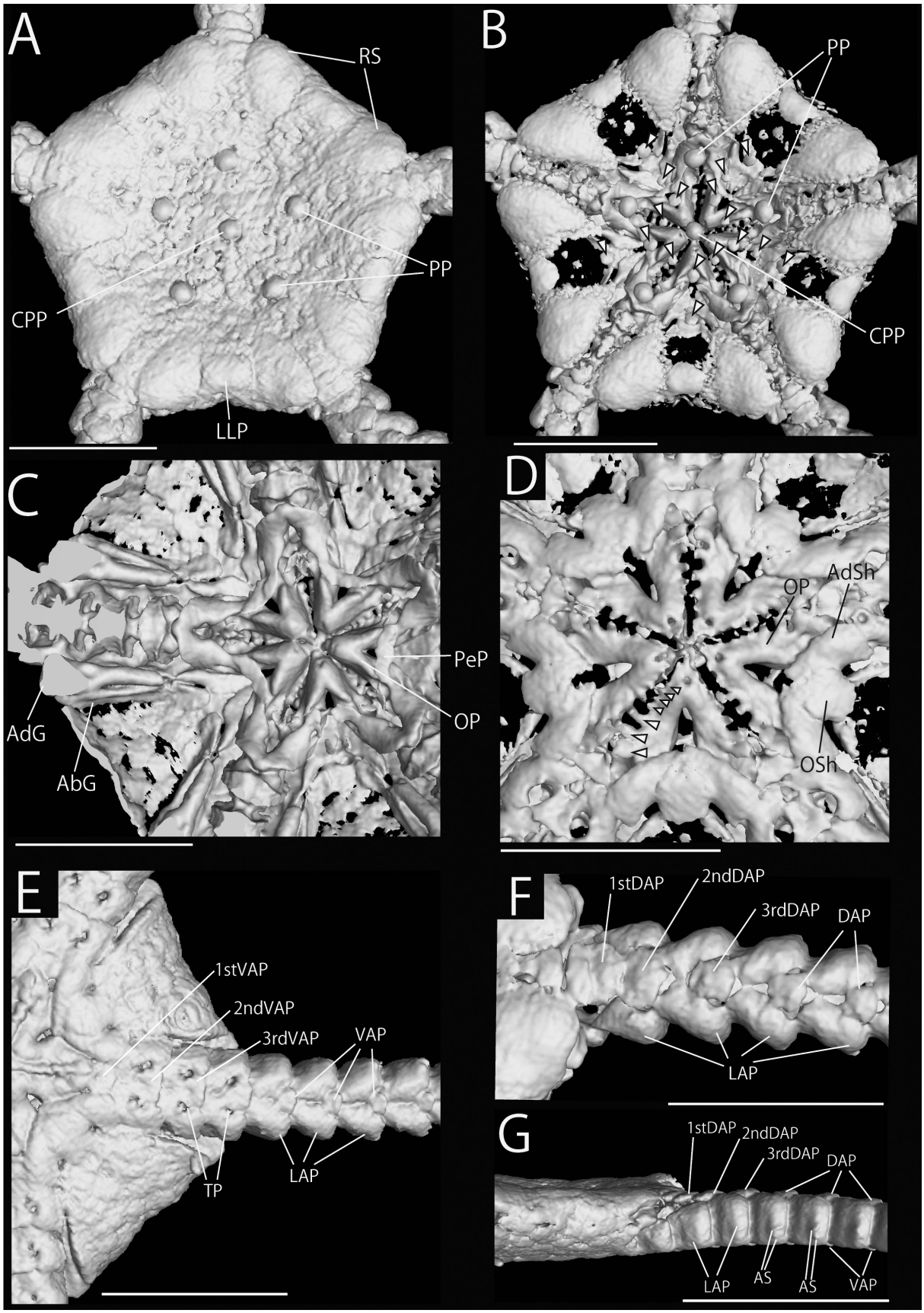

Fig. 4. *Ophiolipus levis*. Micro CT surface rendered images. A, dorsal surface of disc; B, dorsal view of disc plates under the skin. Conspicuously larger hemispherical plates (arrowheads) are radially arranged; C, dorsal view of virtually dissected mouth frame; D, ventral view of ossicles of disc centre, arrowheads denote oral papillae s. l.; E, ventral surface of a part of disc and proximal portion of arm; F, dorsal surface of proximal portion of arm; G, lateral surface of periphery of disc and proximal portion of arm. Abbreviations: AbG, abradial plate; AdG, adradial plate; AdSh, adoral shield; AS, arm spine; CPP, central primary plate; DAP, dorsal arm plate; LAP, lateral arm plate; IMP, interradial marginal plate; OP, oral plate; OSh, oral shield; PeP, peristomial plate; PP, primary plate; RS, radial shield; T, tooth; TP, tentacle pore; VAP, ventral arm plate. Scale bars = 5 mm.

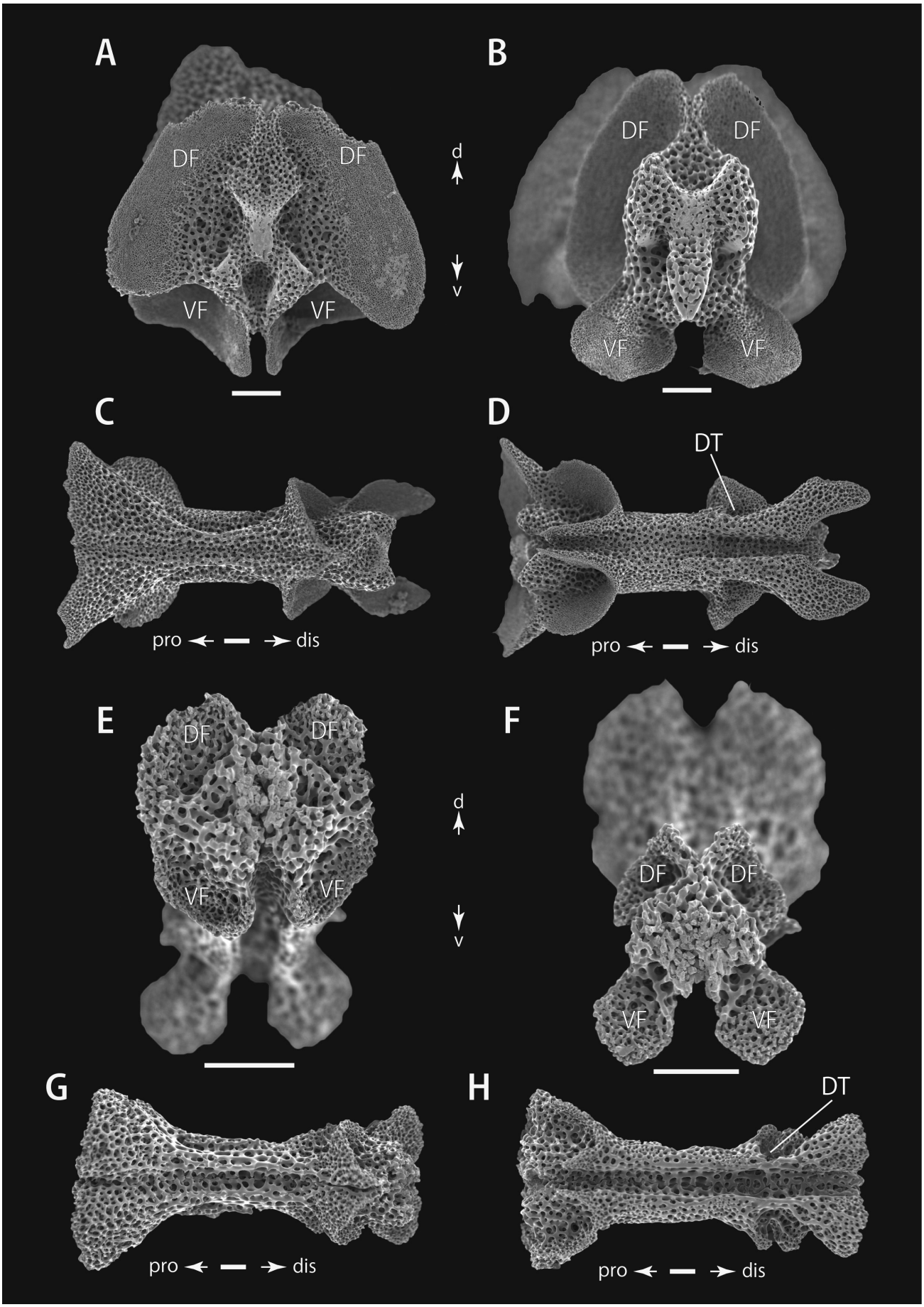

Fig. 5. *Ophiolipus levis*. SEM images of vertebrae. A–D, from proximal portion of arm. E–H, from distal portion of arm. Proximal (A, E), distal (B, F), dorsal (C, G), and ventral (D, H) views. Orientation: d, dorsal; dis, distal; pro, proximal; v, ventral. Abbreviations: DF, dorsal muscle fossae; DT, depression for tentacle; VF, ventral muscle fossae. Scale bars = 100 μm.

0.6 mm in length) (Figs. 2E, 4D). Oral plates triangular, approximately three times longer than wide (1.5 mm in length, 0.4 mm in width) (Figs. 2E, 4D). Oral papillae s.l., 7 to 8 in number, forming a row on abradial ventral edge of oral plate; 5 to 6 inner papillae flat and triangular, and 2 distalmost papillae rectangular, larger than inner ones (Figs. 2E, 4D). Teeth 6 to 7 in number; 3 triangular and spearhead-shaped teeth arranged horizontally at the ventral edge of the dental plates, and 3 to 4 teeth forming a vertical row more dorsally on the dental plates. Only 3 ventralmost teeth visible from outside. Second tentacle pore opening inside the mouth slit (Fig. 2E). Peristomial plates situated on the dorsal side of the 1st vertebra and oral plates, hemispherical, 2 times wider than long (Fig. 4C). Ventral interradii covered by small scales, similar to dorsal scales in shape and size. Gonads round, visible from outside through skin and scales (Fig. 2F). Genital slits narrow, extending from edge of the oral shield almost to disc edge (Fig. 2F). Genital papillae small and flat, forming a row along the adradial and abradial sides of the genital slits (Fig. 2F).

Arms. Five, 1 complete arm 5 mm long and other 4 arms lacking tips (Fig. 2A), twice as wide as length (1.0 mm in width and 0.5 mm in height) in proximal portion, elliptical in transverse section, tapering towards the arm tip (Fig. 2A). Arms entirely covered by thin skin (Figs. 2H, I, 3). On proximal to middle portion of the arm, small granules embedded in skin, similar in shape and size on the dorsal side (Fig. 3A, B); granules disappearing in distal portion of arm (Fig. 3C). Dorsal arm plates separated throughout the arm (Figs. 3A–C, 4B, F). First dorsal arm plate hemispherical, conspicuous, second and following dorsal arm plates kite-shaped and progressively decreasing in size (Fig. 4F). Ventral arm plates separated throughout the arm (Figs. 2H, I, 4D, E). First ventral arm plate conspicuous, triangular with rounded distal edge, second one pentagonal, and more distal plates square and decreasing in size (Figs. 2G–I, 4D, E). Lateral arm plates thick, in contact with each other throughout the arms on both ventral and dorsal surfaces (Figs. 2G–I, 3A–C, 4E, F). Two arm spines, cylindrical with a small acute tip; dorsal one transformed into hook in distal portion of arm (Figs. 3D–F, 4F). The length of arm spines at each tentacle pore is almost the same in most parts of the arm, and the relative lengths to corresponding arm segment are one third on the proximal and one seventh on the distal portion of the arm. First three tentacle pores large, formed by lateral arm plates and ventral arm plates (Figs. 2H, I, 4D, E); fourth and more distal tentacle pores not visible by external observation (Figs. 2H, 3C, F, 4E). Tentacle scales small and flat, two per pore in the first three arm segments (Fig. 4E).

Ossicles. Vertebrae with zygospondylous articulation, dorsal and ventral muscle flanges on both distal and proximal sides (Fig. 5A, B, E, F). Dorsal muscle flanges vertically longer than ventral flanges, which are as long and as wide in proximal portion of arm (Fig. 5A, B) and dorsal ones as large as ventral ones in distal portion of arm (Fig. 5E, F). Longitudinal groove present both on dorsal and ventral sides (Fig. 5C, D, G, H). No canal opening recognisable inside the ventral groove (Fig. 5D, H). Depression for tentacle located at the middle position on the lateral distal side of vertebrae (Fig. 5D, H).

In proximal arm portions, lateral arm plates as long as high, with straight ventral and dorsal edges, slightly convex distal edge, and concave proximal edge (Fig. 6A–C). External side smooth, with a central crescent area composed of more densely meshed stereom (Fig. 6A). Internal side relatively rough meshed stereom than those on external side, with a central ridge composed of more densely meshed stereom (Fig. 6B). A tentacle opening at centre (Fig. 6B). One large nerve tentacle opening and probable one small muscle opening on distal surface (Fig. 6C). In distal arm portions, lateral arm plates rectangular, approximately 1.5 times longer than high (Fig. 6D–F). External view smooth (Fig. 6D). Internal side, with one bar like ridge at central-proximal part and a single tentacle opening at centre (Fig. 6E). One large tentacle opening, one small muscle opening, and another probable muscle opening on distal surface (Fig. 6F).

Arm spines cylindrical, with small acute tip in proximal portion of arm (Fig. 6G), and short, hook-shaped with one secondary tooth in distal portion of arm (Fig. 6H). Dorsal arm plates kite-shaped, with acute proximal angle and obtuse distal angle in proximal portion of arm (Fig. 6J).

Colour. Uniformly creamy white in alcohol. Living colour unknown.

Remarks. *Ophiolipus levis* was described by Koehler (1904). He used "*Ophiolypus*", a misspelling of *Ophiolipus* Lyman, 1878, for describing this species, but *Ophiolipus levis* is the correct name. This species has not been reported upon since Koehler's (1904) original description.

The examined specimen clearly belongs to the family Ophiosphalmidae because of its dorsal and ventral arm plates present along most of the arm, and three between-plate tentacle pores in the most proximal portion of the arms (O'Hara et al., 2018). It falls within the genus *Ophiolipus* by its characteristic feature of having the disc plates covered by thickened skin (Fell, 1960; O'Hara et al., 2018). *Ophiolipus levis* can be distinguished from the two other congeners, *O. agassizii* and *O. granulatus*, mainly based on the arrangement of the granules on the dorsal disc and arms, and in the number of arm spines in the distal portion of the arms. The granules are sparse and separated from each other in *O. levis* (Figs. 2C, 3A, B, D), whereas they are denser and in contact with each other in *O. agassizii* and *O. granulatus* (Lyman, 1878; Koehler, 1897, 1899). One of two arm spines is transformed into hooks in *O. levis* (Figs. 2C, F, 6H), whereas all spines are cylindrical and not hooked in *O. agassizii* and *O. granulatus* (Lyman, 1878; Koehler, 1897, 1899).

Recently, μCT techniques were applied to the examination of few species of ophiuroids (e.g., *Asteronyx loveni* in Okanishi et al., 2017), to elucidate the shapes of ossicles deep inside of the body without destructive dissection. Primary plates and large plates at each interradial disc margin of *Ophiolipus levis* (Fig. 4A), which are a diagnostic character

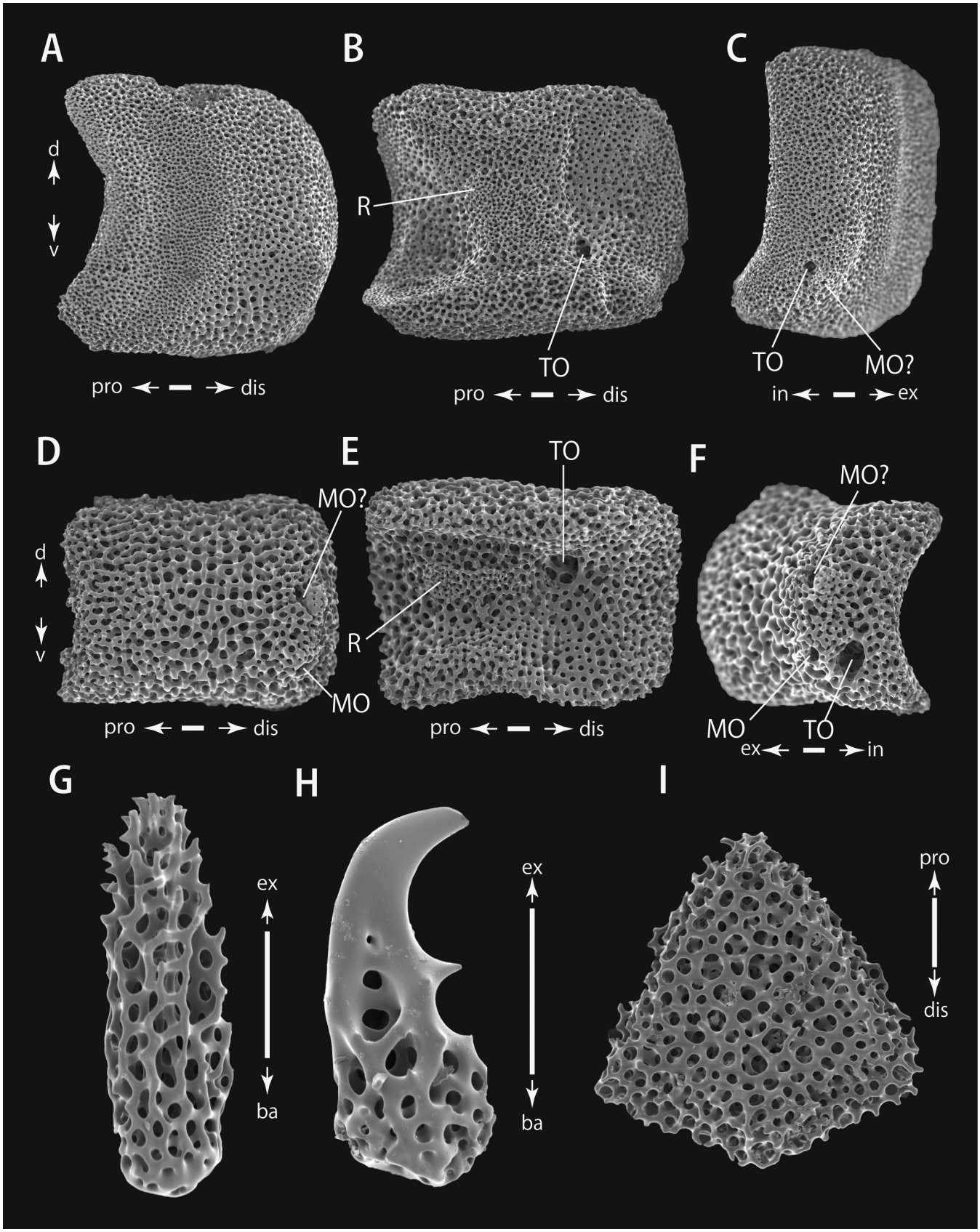

Fig. 6. *Ophiolipus levis*. SEM images of lateral arm plates and arm spines. A–C, lateral arm plates from proximal portion of arm. D–F, lateral arm plates from distal portion of arm (D–F). External (A, D), internal (B, E) and distal (C, F) side. G, H, arm spines from proximal (G) and distal (H) portion of arm. I, dorsal arm plate from proximal portion of arm. Orientation: ba, basal; d, dorsal; in, internal; v, ventral. Abbreviations: MO, muscle opening; P, perforation; R, ridge; TO, tentacle opening. Scale bars = 100 μm.

of Ophiosphalmidae, were clearly observed under the skin by μCT. This non-destructive technique can be a useful tool that can assist in the identification of rare species like *Ophiolipus levis*, of which only few specimens are available for study.

ACKNOWLEDGEMENTS

We are most grateful to Peter Ng, Tan Koh Siang, Dwi Listyo Rahayu, and SJADES 2018 project members for providing us this opportunity to examine the specimens, as well as the captain and crew of KR. *Baruna Jaya VIII* of LIPI for sampling. Specimens were collected under the research permit RISTEKDIKTI 80/SIP/FRP/E5/Dit.KI/III/2018. We are also grateful to Sabine Stöhr of Swedish Museum of Natural History and Ben Thuy of Natural History Museum Luxemburg for greatly improving our manuscript. This work was partly supported by JSPS Core-to-core Program CREPSUM (Collaborative Research and Education Project in Southeast Asia for Sustainable Use of Marine Ecosystems), the grants from the Director-General of National Museum of Nature and Science, "Collaborative research and collection building of marine invertebrates in Southeast Asia developed by the core museum NMNS" and "Imaging of marine invertebrate specimens by micro X-ray computer tomography: its application to taxonomy and building a database of museum specimen images", and KAKENHI Grant Number 17K07549.

LITERATURE CITED

Fell HB (1960) Synoptic key to the genera of Ophiuroidea. Zoology Publications from Victoria University of Wellington, 26: 1–44.

Hendler G (2018) Armed to the teeth: a new paradigm for the buccal skeleton of brittle stars (Echinodermata: Ophiuroidea). Contributions in Science, 526: 189–311.

Koehler R (1897) Échinodermes recueillis par "l'Investigator" dans l'Océan Indien. Les Ophiures de mer profonde. Annales des Sciences Naturelles Zoologie et Paléontologie, 4: 277–372.

Koehler R (1899) Ophiures recueillies par l'Investigator dans l'Ocean Indian. Part I. Les Ophiures de mer profonde. The Trustees of the Indian Museum, Calcutta, 74 pp., 14 pls.

Koehler R (1904) Ophiures de l'Expédition du Siboga. Part I. Ophiures de mer profonde. Siboga-Expeditie, 45b: 1–142.

Lyman T (1878) Ophiuridae and Astrophytidae of the "Challenger" expedition. Part I. Bulletin of Museum of Comparative Zoology, Harvard College, 5(7): 65–168.

Martynov A (2010) Reassessment of the classification of the Ophiuroidea (Echinodermata), based on morphological characters. I. General character evaluation and delineation of the families Ophiomyxidae and Ophiacanthidae. Zootaxa, 2697: 1–154.

O'Hara TD, Stöhr S, Hugall AF, Thuy B & Martynov A (2018) Morphological diagnoses of higher taxa in Ophiuroidea (Echinodermata) in support of a new classification. European Journal of Taxonomy, 416: 1–35.

Okanishi M, Fujita T, Maekawa Y & Sasaki T (2017) Non-destructive morphological observations of the fleshy snake star, *Asteronyx loveni* (Echinodermata: Ophiuroidea: Euryalida) using micro-computed tomography. Zookeys, 663: 1–19.

Okanishi M & Fujita Y (2018) First finding of anchialine and submarine cave dwelling brittle stars from the Pacific Ocean, with descriptions of new species of *Ophiolepis* and *Ophiozonella* (Echinodermata: Ophiuroidea: Amphilepidida). Zootaxa, 4377(1): 1–20.

Stöhr S, O'Hara TD & Thuy B (2012) Global diversity of brittle stars (Echinodermata: Ophiuroidea). PLoS ONE, 7(3): e31940. doi: 10.1371/journal.pone.0031940

Stöhr S, O'Hara T & Thuy B (2020) World Ophiuroidea database. http://www.marinespecies.org/ophiuroidea (Accessed 20 February 2020).

Thuy B & Stöhr S (2016) A new morphological phylogeny of the Ophiuroidea (Echinodermata) accords with molecular evidence and renders microfossils accessible for cladistics. PLoS ONE, 11(5): e0156140. doi: 10.1371/journal.pone.0156140